S. Afr. J. Chem., 2011, **64**, 17–22,
<http://journals.sabinet.co.za/sajchem/>.

Galvanostatic Electrodeposition of Ni-Co Alloys in DMSO under a Magnetic Field

Mehdi Ebadi*, Wan Jeffrey Basirun, Yatimah Alias and Mohammad Reza Mahmoudian

Department of Chemistry, Faculty of Science, University of Malaya, 50603 Kuala Lumpur, Malaysia.

Received 18 February 2010, revised 21 December 2010, accepted 14 January 2011.

ABSTRACT

This paper focuses on the galvanostatic magneto-electrodeposition of Ni-Co alloys in dimethyl sulphoxide (DMSO) in the presence and absence of a permanent parallel magnetic field (PPMF) to the cathode surface. It was found that the mass deposition was enhanced in the presence of PPMF (9 T) compared with the deposition without PPMF. The percentage enhancement potential (ξ%) was elevated (ξ_5% = 23.11, ξ_2% = 10.65, $\xi_{0.5}$% = 4.85) with current densities of 5, 2 and 0.5 mA cm^{-2}, respectively, in the presence of PPMF (9 T). Atomic force microscopy (AFM) showed that the roughness of the Ni-Co alloy films was reduced from 56.187 to 31.716 nm (at 0.2 mA cm^{-2}) and 97.541 to 52.644 nm (at 0.5 mA cm^{-2}) with applied PPMF (9 T) compared with that without the PPMF. The deposited layers were characterized by scanning electron microscopy (SEM), X-ray diffraction (XRD) and energy dispersive X-ray analysis (EDX).

KEYWORDS

Potential enhancement, roughness, DMSO, magnetic electrodeposition.

1. Introduction

Electrodeposition of metals and alloys in aqueous solution is a convenient surface technique in industrial processes. The metal electrodeposition process from an aqueous bath is affected by the hydrogen evolution reaction (HER) and influences the morphology of the electrodeposited surface. Consequently, several researchers[1–4] have reported the electrodeposition of metals in organic solvents in order to avoid the HER and to refine the grain sizes of the electrodeposited layers. Dimethyl sulphoxide (DMSO) is one of the aprotic organic solvents that has been used in electrodeposition of metals.[5–7] The grain sizes of nickel and cobalt were reduced with the enhancement of current density.[8] However, the viscosity of organic solvents is greater than that of aqueous solutions. Consequently, the Helmholtz layers (double layer) in the electrode vicinity are thicker than the double layer of an electrode in aqueous solution. The double layer vicinity of the electrode can be reduced with a permanent parallel magnetic field (PPMF) to the electrode surface.[9,10] The Lorentz force ($\vec{F}_L$) comes from the interaction between magnetic field (B) and electric current (J),[10,11] and that is the most important force for the transport of ions to the electrode surface during the electrodeposition process. The Lorentz force is maximal when the applied magnetic field is parallel to the electrode surface or perpendicular to the current direction.

$$\vec{F}_L = J \times B \quad (1)$$

Equation (2) shows that the limiting current (J_l) increases with an increase of the magnetic field (B):[9,10]

$$j_l = (4.3\times10^3)n^{3/2}A^{3/4}Dv^{-1/4}C^{4/3}B^{1/3} \quad (2)$$

where j_l is the limiting current, ν the viscosity of the solution, C the bulk concentration of electroactive species, B the strength of the magnetic field, D the diffusion constant, A the electrode surface area and n the number of electrons involved in the electron transfer step.

Consequently, the potential gradient (ΔE) is proportional to the current density gradient (ΔJ). The magnetic field could be affected by the morphology of electrodeposited layers. Until now, the electrodeposition of metals in the presence of a magnetic field in organic solvents has not been reported. This paper investigates the electrodeposition of the Ni-Co alloy in the presence and absence of a PPMF (9 T) in DMSO as the solvent at different current densities, where there can be no hydrogen evolution reaction occurring with the alloy electrodeposition. The Ni-Co alloys were electrodeposited by chronopotentiometry (galvanostatic technique).

2. Experimental

The electrodeposition of the Ni-Co alloys in the absence and presence of a PPMF (9 T) was carried out on a copper substrate (0.01 × 1 × 2 cm) by using dried DMSO as the solvent containing $NiCl_2$ (15 g L^{-1}), $CoCl_2$ (3 g L^{-1}) and H_3BO_3 (5 g L^{-1}). The experiments were carried out at different current densities (0.2, 0.5 and 2.5 mA cm^{-2}) using the three electrode setup, at room temperature for 1500 s. The saturated calomel electrode (SCE) was the reference electrode and the nickel and cobalt plates were the counter-electrodes to maintain the concentration of ions. The surface area ratio of nickel to cobalt was 5:1. The cell used for electrodeposition of the Ni-Co alloys in the presence and absence of the PPMF (9 T) was made from Teflon (10 × 6 × 3 cm). The distance between the cathode and anode plates was 4.5 cm. The magnetic field was placed perpendicular to the current flow direction as shown in Fig. 1. Before the electrodeposition process, nitrogen gas was bubbled through the solution for 20 min in order to remove dissolved oxygen. Also, before electroplating, the copper plates were activated and chemically polished by mixed acids (HCl + H_2SO_4 + CrO_3 + HNO_3) for a few seconds and then rinsed with distilled water. The topography of the deposited layers was investigated *via* atomic force microscopy (AFM PS 3000-NS3a, Digital Instruments, Santa Barbara, CA, USA). The nickel electrodeposits were analyzed by using an

* To whom correspondence should be addressed. E-mail: mehdi_2222002@yahoo.com

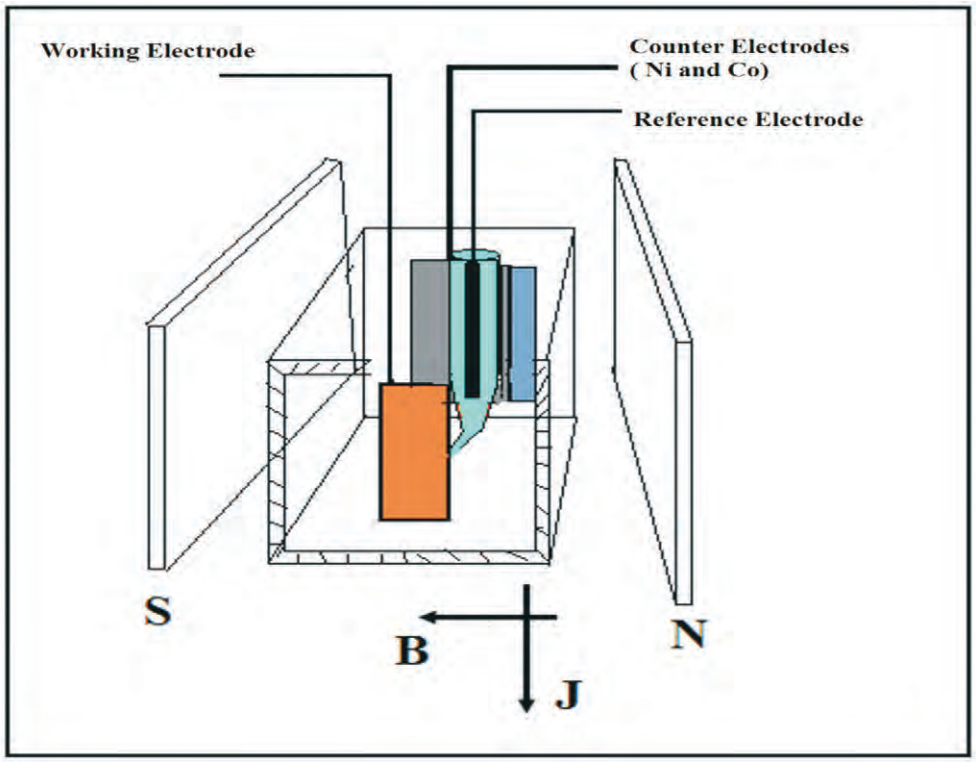

Figure 1 Schematic diagram of the experimental set up using a Teflon cell (10 × 3 cm) copper cathode plate (2 × 1 cm) and Ni anode. The copper face was parallel to the magnetic flux (9 T).

X-Ray diffraction (D_8-Advanced XRD) instrument (Bruker Malaysia SDN Bhd) set with Cu K_α radiation of wavelength 1.540 Å. The mass electrodeposited was determined from the difference in mass between the bare and coated Cu plates. Scanning electron microscopy (SEM-FEI Quanta 200F, FEI Company, Hillsboro, OR, USA) was used to capture images of the surface morphology of the electrodeposited samples and it also included energy dispersive X-ray (EDX) analysis acquired with an INCA Energy 400 energy dispersive system. Chronopotentiometry experiments were performed with an Autolab PGSTAT-302N potentiostat/galvanostat (Metrohm Autolab Company, Utrecht, Netherlands), which was equipped with GPES software.

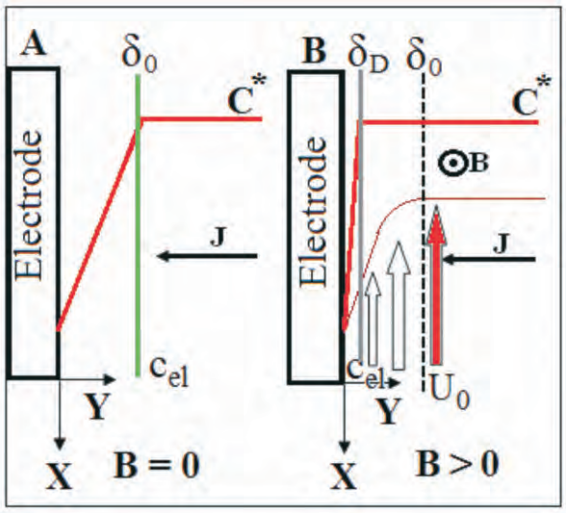

Figure 2 Schematic illustration of the mechanism of enhanced mass transport of charged electro-active species under an applied magnetic field (where U_0 is the bulk stream, C* is the bulk and C_{el} is the surface concentration of electroactive species at the electrode).

3. Results and Discussion

3.1. Mass Electrodeposited

The movement of ions can be enhanced by increasing the current density to the electrode surface from the bulk solution. Consequently, the mass electrodeposited increased with an increase in current density. This has been reported by numerous researchers.[12–14] The Lorentz force ($\vec{F}_L$) is the main force that transports ions from the bulk solution to the electrode surface when a magnetic field is placed perpendicular to the current flow direction. The interaction of the magnetic field aligned parallel to the cathode surface with the current flow to the cathode surface results in the Lorentz force ($\vec{F}_L = J \times B$). According to Hinds *et al.*,[11] the Lorentz force has the largest contribution among all the forces present in the magneto-hydrodynamic (MHD) effect towards the mass transport increase. The influence

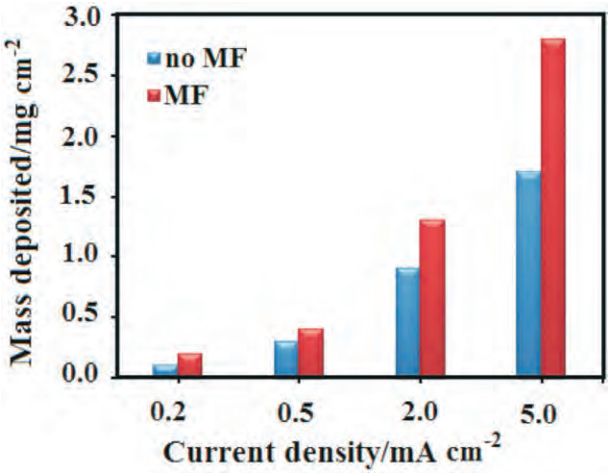

Figure 3 The amount of Ni-Co alloy electrodeposited in the presence and absence of the PPMF (9 T) for 1500 s at various current densities.

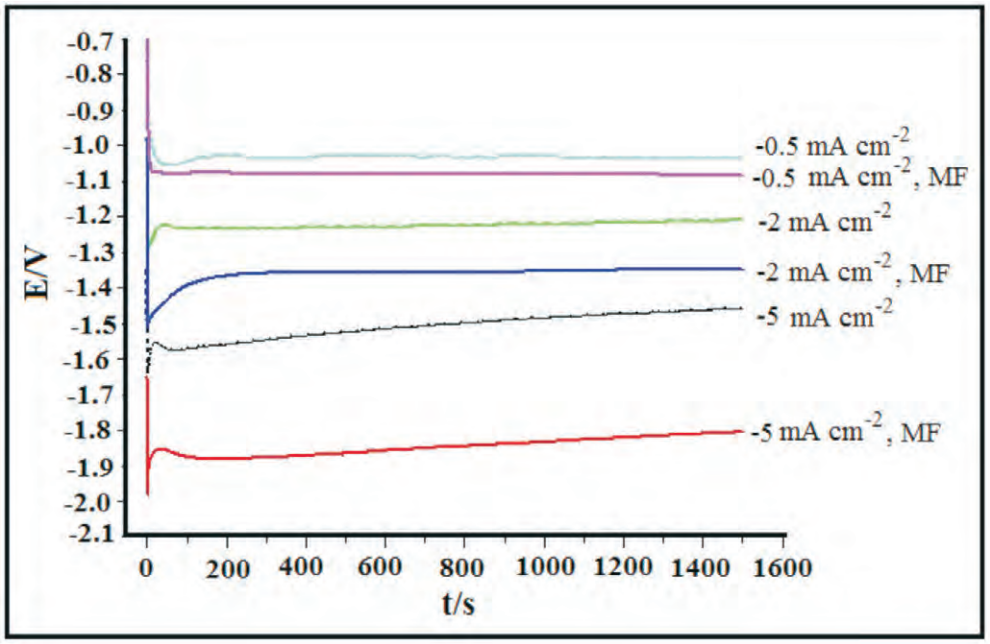

Figure 4 Chronopotentiometry of Ni-Co alloys deposited in the presence and absence of a PPMF (9 T) at different current densities.

of the magnetic field on the motion of ions and the thickness reduction of the diffusion layer is depicted schematically in Fig. 2. It is observed that the normal diffusion layer δ_0 could be diminished to a narrow layer δ_D, due to the magnetic field induction while the magnetic flux (B) and electric current (J) were parallel and perpendicular to the surface of the cathode, respectively.[15] Therefore, the MHD effect (caused largely by the Lorentz force) reduces the diffusion layer thickness, thus increasing the mass transport to the electrode surface. The graph shown in Fig. 3 illustrates that the mass of the Ni-Co alloy deposited in DMSO increased due to the effect of the PPMF (9 T) at various applied current densities. From Fig. 3, there is an increase of the mass electrodeposited in the presence of the PPMF (9 T) compared with that without the PPMF, and the difference between the mass electrodeposited in the presence of the PPMF and without PPMF was enhanced with an increase in the current density. Thematically, the Lorentz force ($\vec{F}_L$), which is greater at higher current density (Eq. 1), gave more mass deposited at higher current densities (0.2 to 5 mA cm^{-2}) as can be seen in Fig. 3. However, the chronopotentiometry diagrams (Fig. 4) of the electrodeposition of the Ni-Co alloys show that the potential (*vs.* SCE) is enhanced in the presence of the PPMF. Figure 4 also raises another important point, that with the increase of current density the difference between the electrical potential in the absence and presence of the PPMF (9 T) is increased ($E_{MF} - E_{no\ MF}$ for $5 > 2 > 0.5$ mA cm^{-2}). Ohm's law is expressed as $E = IR$. The $|E|$ increases with an increase of $|I|$ in the same solution. The overall rate of electrode reaction at the potentials from $|E| = -1.497$ to -1.84, -1.22 to -1.35 and -1.03 to -1.08 V *vs.* SCE increases in the presence of the PPMF. The enhancement could be expressed as a percentage according to following formula:[16]

$$\xi\% = \frac{\Delta E}{E_i} \times 100$$

where ΔE is the difference of potential obtained in the presence and absence of the PPMF (9 T) and E_i is the potential without a PPMF. The percentage enhancement potential (%) was calculated as ($\xi_5\% = 23.11$, $\xi_2\% = 10.65$ and $\xi_{0.5}\% = 4.85$) at current densities of 5, 2 and 0.5 mA cm^{-2}, respectively.

3.2. X-ray Diffraction (XRD) Studies

The Ni-Co alloy surface was analyzed by XRD (Fig. 5). The XRD diffraction peaks of the deposited layers were procured from a scan of 2θ values from 40 ° to 95 °. The intensity of (311) for the electrodeposited layers without the PPMF is lower than the intensity of (311) from the electrodeposited layers with the presence of the PPMF (9 T). The intensities and full widths at half maximum (FWHM) of (220) and (200) from the electrodeposited Ni-Co alloys in the presence of the PPMF were increased at various current densities. Consequently, it was found that the PPMF had affected the texture and morphology of the Ni-Co alloy electrofabricated in DMSO solution. Notably, the growth of small grain sizes with (200) was elevated in the presence of the PPMF (9 T) through the magneto-electrodeposition in dimethyl sulphoxide. The evidence of these changes observed through the AFM and SEM images is that the electrodeposited layers in the presence of a PPMF are more uniform compared with the electrodeposited layers in the absence of a PPMF (this aspect will be discussed later). These changes in texture of the electrodeposits in the presence of a PPMF are due to the increased transport of ions from the bulk solution to the electrode surface through the reduction of the Nernst diffusion layer thickness. Furthermore, the planes have not shifted while a PPMF was applied. It means that the structure of the electrodeposited layers could not be changed by using a magnetic field.

3.3. Atomic Force Microscopy (AFM)

Figure 6 shows the AFM images from the surface of the Ni-Co alloy electrodeposited in DMSO and the determination of the surface roughness. The surface roughness ($R_g(L)$) of an L × L area could be calculated in terms of the root mean square (rms) value defined as:[16]

$$R_g(L) = \sqrt{\sum_i^n \frac{(\bar{h} - h_i)^2}{n}} \qquad (3)$$

where n is the number of points measured across a surface L × L, $\bar{h}$ is the average height and h_i is the height of each point. The applied PPMF (9 T) on the electrode gave a smoother electrodeposited surface. As mentioned before, the magnetic flux (B) decreases the Nernst diffusion layer (δ_D) during the electro-

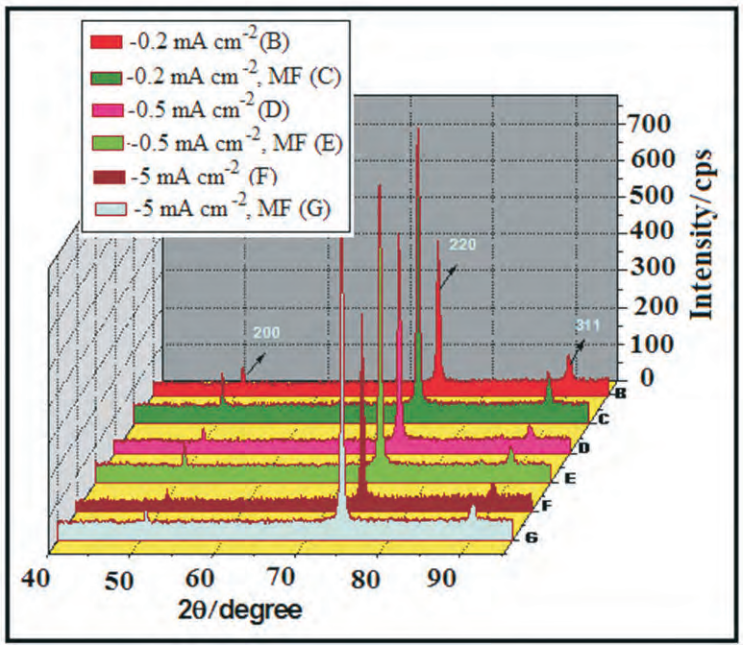

Figure 5 XRD spectra of the Ni-Co layers electrodeposited with and without a PPMF at different current densities.

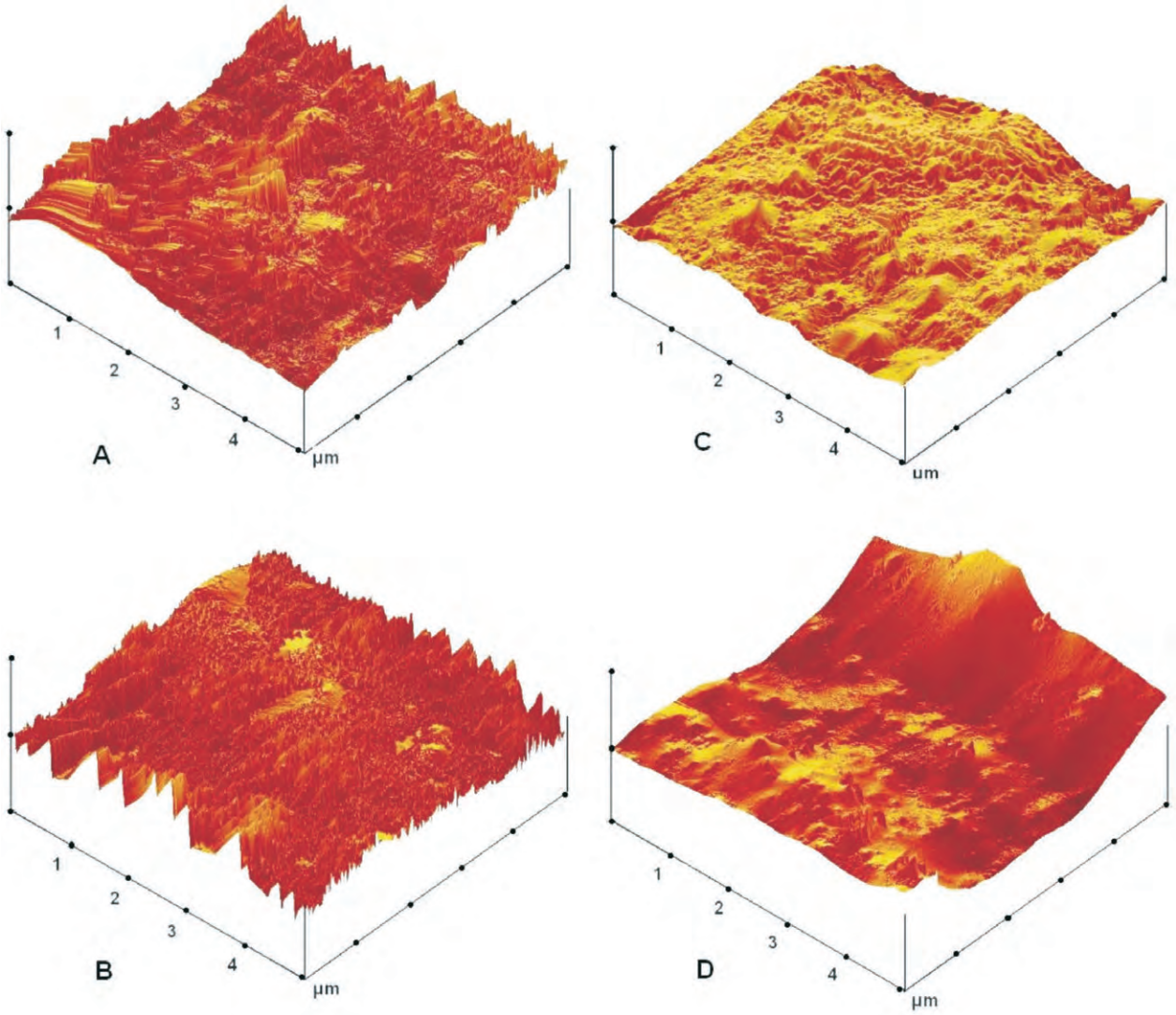

Figure 6 AFM images of the Ni-Co films electrodeposited in the absence of PPMF: (**A**) 0.2 mA cm^{-2}, (**B**) 0.5 mA cm^{-2}, and in the presence of a PPMF (9 T): (**C**) 0.2 mA cm^{-2}, (**D**) 0.5 mA cm^{-2}.

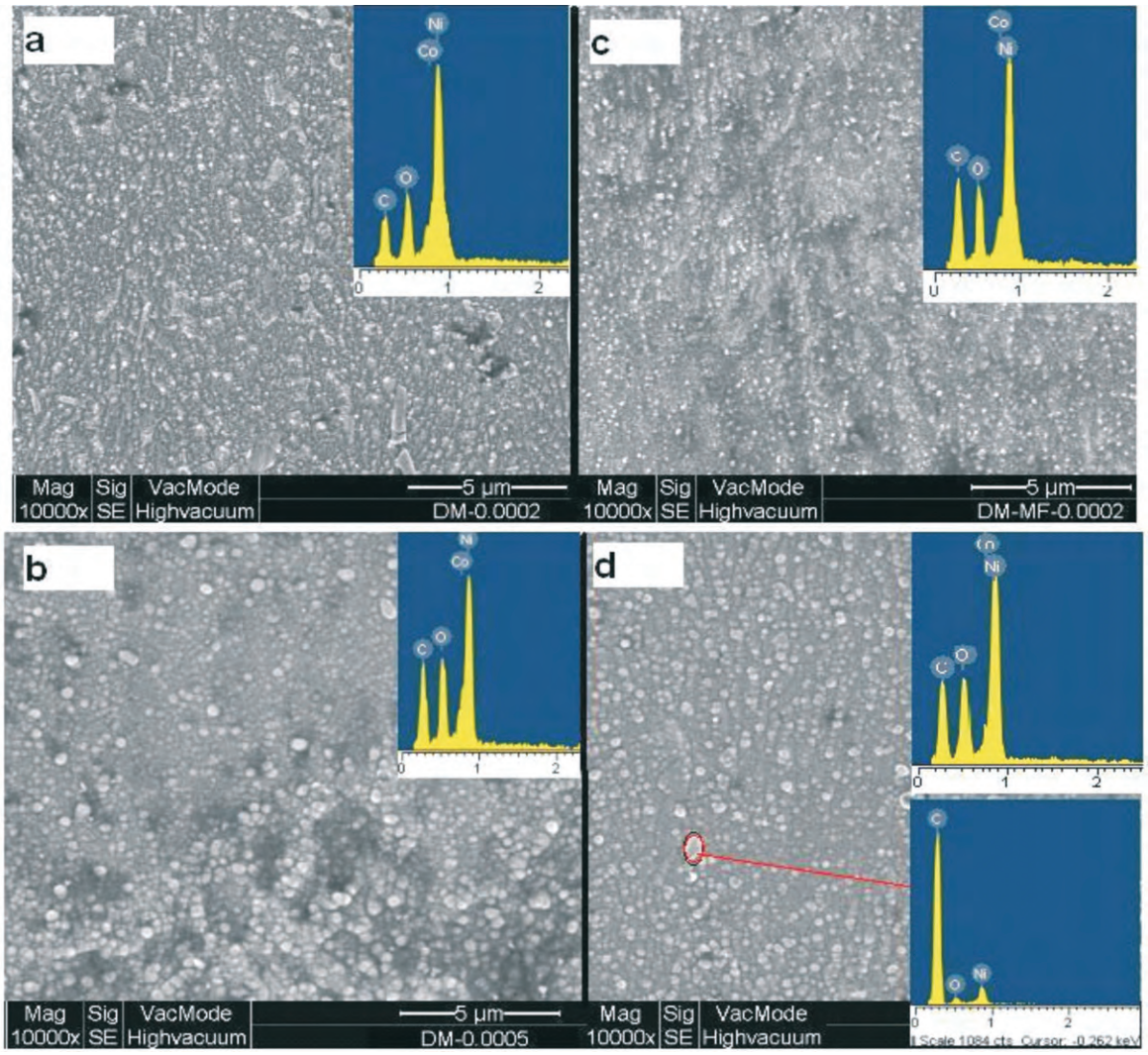

Figure 7 SEM/EDX micrographs of Ni-Co electrodeposited without PPMF: (**a**) 0.2 mA cm^{-2}, **(b)** 0.5 mA cm^{-2}, and with PPMF (9 T): (**c**) 0.2 mA cm^{-2}, **(d**) 0.5 mA cm^{-2}.

deposition process. This causes the electrodeposition to occur in a more uniform manner when the PPMF is applied.

At a current density of 0.2 mA cm^{-2}, the roughness factor was reduced from 56.187 nm (without PPMF) to 31.716 nm (with PPMF), whereas at a current density of 0.5 mA cm^{-2}, the roughness factor was reduced from 97.541 nm (without PPMF) to 52.644 nm (with PPMF) in DMSO solvent. Matsushima *et al.*[17] have also investigated the influence of a magnetic field on the atomic arrangement during the electrodeposition process. Dendrite formation on the electrodeposited surface was reduced in the presence of a PPMF and can be seen in the AFM images in Fig. 6. Images 6A and 6B were prepared at 0.2 and 0.5 mA cm^{-2} in the absence of a PPMF whereas images 6C and 6D were obtained in the presence of a PPMF at the same current densities. The elemental components in each sample were obtained by using energy dispersive X-ray analysis (EDX). Notably, the decomposition of the organic solvent (DMSO) took place with an increase in the current density as well as the applied PPMF during the electrodeposition at higher potentials. The white spots are carbon deposited due to the decomposition of DMSO (Fig. 6D). One of the main disadvantages of using an organic solvent is the limited potential window in the electrodeposition process. The decomposition of DMSO with PPMF (9 T) was greater than that without the PPMF, due to the increased potential in the electrodeposition process (Table 1). Watanabe[8] has noted that the structure of plated films is determined by the type of elements and their composition.

3.4. Scanning Electron Microscopy (SEM)

Two types of Ni-Co alloy surfaces were chosen for the SEM characterization, and they were produced from the electrodeposits with and without a PPMF in the DMSO solvent. Figure 7 shows the images of the Ni-Co alloy electrodeposited at 0.2 and 0.5 mA cm^{-2}. The SEM images (7a, 7b) and (7c, 7d) show the Ni-Co alloys that were prepared at 0.2 and 0.5 mA cm^{-2} in the absence and presence of the PPMF (9 T) respectively. From the SEM images, it can be seen that the electrodeposited surfaces with the PPMF are more uniform compared with the electrodeposited surfaces without the PPMF. This also conforms with our previous results[12,13,18] and those of Ispas *et al.*[19,20] Carbon deposit was also observed on the surface layers in the EDX spectrum where it was marked on the SEM images as white spots (see Fig. 7d). It was produced from the decomposition of the DMSO molecules at higher potentials from higher electrodeposition current densities. The elemental components in each sample were obtained by using energy dispersive X-rays (EDX) and are shown in Table 1. The cobalt electrodeposited was enhanced with applied PPMF at different current densities. The EDX spectra are shown together with the SEM images in Fig. 7. From the EDX results, normal electrodeposition has taken place.

Table 1 Percentage of each element electrodeposited with and without the PPMF at current densities of 0.2 and 0.5 mA cm^{-2}.

Current density	C%	O%	Ni%	Co%
0.2 mA cm^{-2} without PPMF	10.48	10.81	78.31	0.4
0.2 mA cm^{-2} with PPMF	9.26	9.8	79.61	1.33
0.5 mA cm^{-2} without PPMF	11.31	10.95	75.35	2.39
0.5 mA cm^{-2} with PPMF	11.48	11.03	62.93	14.56

Therefore the concentration of electrodeposited elements is proportional to the concentration of metal ions in solution and the anomalous behaviour did not appear during the electrodeposition. The anomalous behaviour refers to the fact that the less noble metal (i.e. Co) is preferentially deposited compared with the more noble metal (i.e. Ni). Our previous reports[15] showed that the anomalous behaviour could be explained by the hydrogen suppressed mechanism (HSM) when using water as the solvent. However, the anomalous electrodeposition occurred when dried DMSO (water free) was used as the solvent.

Conclusions

The influence of a magnetic field (9 T) with parallel orientation to the electrode surface on the electrodeposition of Ni-Co alloys was studied in DMSO solvent at room temperature. The PPMF influenced the electrochemical reaction by reducing the Nernst diffusion layer thickness, thus the limiting current density and the mass deposition were increased. Consequently, the electrode potential (*vs.* reference) was increased with an increase of current density and hence the mass of alloy electrodeposited increased in the presence of the PPMF. Furthermore, with increase of current density the percentage enhancement potential (%ξ) was increased (%ξ_5 = 23.11, %ξ_2 = 10.65 and %$\xi_{0.5}$ = 4.85) at 5, 2 and 0.5 mA cm^{-2}, respectively, in the presence of the PPMF. The roughness of the Ni-Co alloy films electrodeposited on the copper plates decreased (56.187 to 31.716 nm and 97.541 to 52.644 nm) with applied PPMF at 0.2 and 0.5 mA cm^{-2}, respectively. From the AFM, dendrite formation on the electrodeposited surface decreased with the applied PPMF as well.

Acknowledgements

We thank the University of Malaya for financial support from University research grant PS 388/2008C and UMCiL grant (TA2009/2008A). One of the authors (Mehdi Ebadi) is thankful for a fellowship from the University of Malaya.

References

1 E. Pál and I. Dékány, *Col. Sur. A,* 2008, **318**, 141–150.
2 P. Heoa, R. Ichino and M. Okido, *Electrochim. Acta,* 2006, **51,** 6325–6330.
3 J. Fu, D. Gao, Y. Xu and D. Xue, *Electrochim. Acta,* 2008, **53**, 5464–5468.
4 P. Liu, Q. Yang, Y. Tong and Y. Yang, *Electrochim. Acta,* 2000, **42**, 2147–2152.
5 G. Li, Y. Tong and G. Liu, *J. Electroanal. Chem.*, 2004, **562**, 223–229.
6 M.C. Lefebvre and B.E. Conway, *J. Electroanal. Chem.*, 2000, **480**, 34–45.
7 G.-R. Li, Q.-F. Ke, G.-K. Liu, P. Liu and Y.-X. Tong, *Mat. Lett.*, 2007, **61**, 884–888.
8 T. Watanabe, *Nano-Plating,* Elsevier Science, Oxford, UK, 2004, pp. 163–170.
9 O. Lioubashevski, E. Katz and I. Willner, *J. Phys. Chem. C,* 2007, **111**, 6024–6032.
10 O. Lioubashevski, E. Katz and I. Willner, *J. Phys. Chem. C,* 2004, **108**, 5778–5784.
11 G. Hinds, J.M.D. Coey and M.E.G. Lyons, *Electrochem. Comm.*, 2001, **3**, 215–218.
12 M. Ebadi, W.J. Basirun and Y. Alias, *Asian J. Chem.*, 2009**, 21,** 7354–7362.
13 M. Ebadi, W.J. Basirun and Y. Alias, *Asian J. Chem.*, 2009, **21**, 6343–6353.
14 A. Ispas, H. Matsushima, W. Plieth and A. Bund, *Electrochem. Acta,* 2007, **52**, 2785–2795.
15 M. Ebadi, W.J. Basirun, Y. Alias and M. R. Mahmoudian, *Chem. Cent. J.*, 2010, **4**, 14.
16 I. Tabakovic, S. Riemer, V. Vas'ko, V. Spozhnikov and M. Kief, *J. Electrochem. Soc.*, 2003, **150**, C635–C640.
17 H. Matsushima, T. Nohira, I. Mogi and Y. Ito, *Sur. Coat. Tech.*, 2004, **179**, 245–251.
18 M. Ebadi, W.J. Basirun and Y. Alias, *J. Chem. Sci.,* 2009, **112,** 279–285.
19 A. Ispas, H. Matsushima, A. Bund and B. Bozzini, *J. Electroanal. Chem.*, 2009, **626**,174–182.
20 J.A. Koza, M. Uhemann, C. Mickel, A. Gebert and L. Schultz, *J. Mag. Mat.*, 2009, **321**, 2265–2268.